

**A novel unsupervised bee colony optimization (UBCO) method for remote sensing image classification: A case study in a heterogeneous marsh area**

Journal:	<i>International Journal of Remote Sensing</i>
Manuscript ID	TRES-PAP-2015-0487.R5
Manuscript Type:	IJRS Research Paper
Date Submitted by the Author:	18-Sep-2016
Complete List of Authors:	Li, Huapeng; Northeast Institute of Geography and Agroecology, Chinese Academy of Sciences, Zhang, Shuqing; Northeast Institute of Geography and Agroecology, Chinese Academy of Sciences, Ding, Xiaohui; Northeast Institute of Geography and Agroecology, Chinese Academy of Sciences, ; University of Chinese Academy of Sciences, Zhang, Ce; Lancaster University, Lancaster Environment Centre Cropp, Roger; Griffith University, Griffith School of Environment
Keywords:	classification, algorithm, remote sensing
Keywords (user defined):	bee colony optimization, swarm intelligence

SCHOLARONE™  
Manuscripts

# A novel unsupervised bee colony optimization (UBCO) method for remote sensing image classification: A case study in a heterogeneous marsh area

Huapeng Li<sup>a\*</sup>, Shuqing Zhang<sup>a</sup>, Xiaohui Ding<sup>a,b</sup>, Ce Zhang<sup>c</sup>, Roger Cropp<sup>d</sup>

<sup>a</sup>*Northeast Institute of Geography and Agroecology, Chinese Academy of Sciences, Changchun, 130012, China;* <sup>b</sup>*University of Chinese Academy of Sciences, Beijing, 100049, China;* <sup>c</sup>*Lancaster Environment Centre, Lancaster University, Lancaster LA1 2YQ, UK;* <sup>d</sup>*Griffith School of Environment, Griffith University, Gold Coast, 4222, Australia*

\*Corresponding author. Email: lihuapeng@neigae.ac.cn

Unsupervised image classification is an important means to obtain land use/cover information in the field of remote sensing, since it does not require initial knowledge (training samples) for classification. Traditional methods such as *k*-means and ISODATA have limitations in solving this NP-hard unsupervised classification problem, mainly due to their strict assumptions about the data distribution. The bee colony optimization (BCO) is a new type of swarm intelligence, based upon which a simple and novel unsupervised bee colony optimization (UBCO) method is proposed for remote sensing image classification. UBCO possesses powerful exploitation and exploration capacities that are carried out by employed bees, onlookers and scouts. This enables the promising regions to be globally searched quickly and thoroughly, without becoming trapped on local optima. In addition, it has no restrictions on data distribution, and thus is especially suitable for handling complex remote sensing data. We tested the method on the Zhalong National Nature Reserve (ZNNR)—a typical inland wetland ecosystem in China, whose landscape is heterogeneous. The preliminary results showed that UBCO (overall accuracy = 80.81%) achieved statistically significant better classification result (McNemar test) in comparison with traditional *k*-means (63.11%) and other intelligent clustering methods built on genetic algorithm (UGA, 71.49%), differential evolution (UDE, 77.57%) and particle swarm optimization (UPSO, 69.86%). The robustness and superiority of UBCO were also demonstrated from the two other study sites next to the ZNNR with distinct landscapes (urban and natural landscapes). Enabling to consistently find the optimal or nearly optimal global solution in image clustering, the UBCO is thus suggested as a robust method for unsupervised remote sensing image classification, especially in the case of heterogeneous areas.

## 1. Introduction

Land use/cover data is very important for diverse disciplines including ecology, geography, climatology, etc. (Lu and Weng 2007, Huang and Laffan 2009, Otukei and Blaschke 2010). For example, it is required in a lot of ecological applications such as assessing species

1  
2  
3 distributions modeling and carbon stocks estimation (Kerr and Ostrovsky 2003, Jain and Yang  
4 2005). Remote sensing has been recognised as an efficient tool to acquire land use/cover  
5 information because of its unique advantages including synoptic view, multi-temporal  
6 coverage and cost-effectiveness. Scientists and practitioners have put substantial efforts into  
7 the field of remote sensing image classification and a number of methods have been described  
8 (Melgani and Bruzzone 2004, Bagan *et al.* 2005, Fisher 2010). However, an accurate remote  
9 sensing classification is still of a great challenge due to the complexity of remote sensing data  
10 (Guerschman *et al.* 2003).

11  
12  
13 Generally, there are two types of classification methods, supervised and unsupervised.  
14 Supervised methods such as maximum likelihood classifiers can generate good results in  
15 various kinds of applications (Melgani and Bruzzone 2004, Wright and Gallant 2007, Adam *et*  
16 *al.* 2014). Such methods, however, require prior knowledge (training samples) to guide the  
17 classification, and the classification results rely heavily on the number and quality of training  
18 samples (Chuvieco and Congalton 1988). The collection of training samples can be rather  
19 time-consuming and labour intensive (Duda and Canty 2002). Without prior definition and  
20 knowledge, unsupervised methods classify images utilise only the statistical information  
21 inherent the image (Cihlar *et al.* 1998). Therefore, they are superior to the supervised  
22 approaches for applications where the user has little prior knowledge about the available data  
23 (Li *et al.* 2016). Because of their simplicity and efficiency, unsupervised methods have been  
24 widely used in a variety of remote sensing applications (Xiao *et al.* 2002, Miller and Yool  
25 2002, Schmid *et al.* 2004, Bartholomé and Belward 2005).

26  
27  
28  
29  
30  
31  
32  
33  
34  
35  
36  
37  
38  
39  
40  
41  
42  
43  
44  
45  
46  
47  
48  
49  
50  
51  
52  
53  
54  
55  
56  
57  
58  
59  
60  
*k*-means, in which a fixed class number is employed, is one of the most commonly used  
methods for unsupervised image classification. The method starts with a number of arbitrary  
centres, usually chosen from the image pixels; then each pixel is assigned to the centre nearest  
to the pixel. Subsequently, each centre is recalculated as the mean of all pixels classified to it.  
The assignment and centre recalculation steps are repeated until a predefined termination  
condition is satisfied (Jain 2010). While ISODATA, a variation of *k*-means, is another  
frequently used method which adjusts the class number during program execution (Goncalves  
*et al.* 2008). In spite of its simplicity and ease of application, *k*-means exhibits some  
shortcomings that can seriously affect its classification result:

- (1) sensitivity to the initial conditions (Khan and Ahmad 2004),
- (2) inability to reach the global optimal solution (Jain 2010), and
- (3) requirement to the distribution of available data (Shah *et al.* 2004).

The rapid development of artificial intelligence provides new opportunities in the field of  
remote sensing classification, and several 'intelligent' algorithms, such as genetic algorithm  
(GA) and ant colony optimization (Liu *et al.* 2008, Pal 2008) have been introduced. GA is a  
commonly used and typical intelligent algorithm in the field of image classification (e.g.  
Maulik and Bandyopadhyay 2000), which transforms image classification to an optimization  
problem. Initially, a population of candidate solutions is created randomly and each solution is  
viewed as a chromosome. Solutions are then chosen for reproduction by a selection operator  
according to their fitness; these selected solutions are further refined by crossover and  
mutation operators when breeding to produce the next cycle; the iteration continues until a  
predefined termination criteria is met. Two other intelligent algorithms that draw increasing  
attention among researchers of different disciplines are differential evolution (DE) (Storn and

1  
2  
3 Price 1995, Price *et al.* 2005) and particle swarm optimization (PSO) (Eberhart and Kennedy  
4 1995). DE employs the same three operators (crossover, mutation and selection) as GA, to  
5 improve the population of candidate solutions. But, different from GA, the chance being  
6 selected as parents is equal for all solutions in DE. Each solution produces a mutant (mutation)  
7 which then competes with its parent: the better one (with higher fitness) wins the competition  
8 (crossover). As for PSO, the optima in a solution space is found by simulating the social  
9 behaviour of bird flocking and fish schooling. Here, positions (possible solutions of the  
10 problem) of a population of particles are changed according to the current optimum particles  
11 in each iteration. As a result, good information spreads through the population, which leads  
12 the particles towards good areas, i.e. searching for the optimal solution.

13  
14 Recently, bee colony optimization (BCO), a new type of swarm intelligence, has been  
15 successfully applied to diverse fields such as numerical function optimization (Karaboga and  
16 Basturk 2007), data mining (Shukran *et al.* 2011) and image processing (Hornig 2011).  
17 Previous studies have demonstrated that BCO can outperform other intelligent methods in  
18 searching for an optimal solution (Karaboga and Basturk 2008, Karaboga and Akay 2009) and  
19 can solve complex NP-hard problems (Non-deterministic Polynomial  
20 hard computational problems that cannot be solved in polynomial time; these problems are  
21 some of the most difficult problems to solve in computing, as increases in computing power  
22 can provide only marginal benefits) such as the travelling salesman problem (Karaboga and  
23 Basturk 2008, Wong *et al.* 2010). However, few attempts have been made to apply this  
24 promising method to unsupervised remote sensing classification, which belongs to the family  
25 of NP-hard problems (Admane *et al.* 2006). Banerjee *et al.* (2012) and Deriche and Fizazi  
26 (2015) respectively proposed two BCO-based unsupervised image classification methods, in  
27 which the image was classified pixel by pixel through judging the belonging of neighborhood  
28 pixels of the classified pixels. The two methods are therefore dependent on expert knowledge  
29 to some extent, and do not consider the general characteristics of the image.

30  
31 The objective of this paper is to propose a novel unsupervised bee colony optimization  
32 (UBCO) method for image classification based on BCO. UBCO was tested with three  
33 different landscapes located within or surrounding the Zhalong National Nature Reserve,  
34 China, a typical complex and heterogeneous inland wetland area. The performance of the  
35 proposed method was compared with traditional *k*-means and three intelligent classification  
36 methods built on the above-mentioned GA, DE and PSO. To the best of our knowledge, this is  
37 the first application of this method to the completely unsupervised image classification  
38 problem.

## 39 40 41 42 43 44 45 46 47 **2 Bee colony optimization (BCO)**

48  
49 BCO simulates the behaviours of real bees in the process of seeking the best food source  
50 when collecting nectars. It has been discovered that bees in colonies consist of three groups:  
51 employed bees, onlookers and scouts, of which the latter two groups are called unemployed  
52 foragers. When seeking food, bees communicate with each other through a waggle dance  
53 performed in the dancing area of a hive (Karaboga and Basturk 2007). A bee that has found a  
54 food source (employed bee), will share information about the location of the food supply with  
55 onlookers (with a certain probability of effective communication) through the waggle dance.

After watching the waggle dance on the dancing floor, an onlooker will choose to follow the employed bee with the most profitable food source. The more profitable food sources are chosen with a greater probability by the onlookers because much more information about these sources is propagated. Recruitment is therefore proportional to the profitability of the food source (Karaboga *et al.* 2014), and a bee colony maximises its profit through this mutual cooperation behaviour among individuals.

Figure 1 is here

The process by which a bee colony seeks food is illustrated by Figure 1, in which a “Hive” consists of “Waggle dance area” (for employed bees sharing food source information), “Nectar A” (a discovered food source), and “Unknown nectar” (a possible food source). In the beginning, a potential forager has no knowledge about the food sources around the nest. At this time, she has two possible options: one is to be a ‘scout’ and start searching for a food source near the nest randomly (route ‘S’ in Figure 1). The other is to be recruited after watching the waggle dances and then begin searching for a food source (route ‘R’ in Figure 1). After finding a food source, the forager is employed and returns to the hive with food information (i.e. nectar position and amount). After unloading the food, the employed forager may become an uncommitted follower (route ‘UF’) by abandoning the current food source, or dance to recruit potential foragers (route ‘EF1’), or return to the food source directly without recruiting bees (route ‘EF2’).

### 3 Unsupervised bee colony optimization (UBCO) method

The UBCO method was developed from the BCO, and is proposed for unsupervised remote sensing image classification. Figure 2 briefly illustrates the procedure of UBCO for unsupervised remote sensing image classification, details of which will be provided in the following sections.

Figure 2 is here

**3.1 Basic principle.** Suppose an image consists of  $N$  pixels with  $n$  attributes and  $m$  classes for classification. UBCO identifies the image by determining a fixed number ( $m$ ) of optimal cluster centres ( $C_1, C_2, \dots, C_m$ ) to minimise the clustering metric. The clustering metric ( $M$ ) is the sum of the Euclidean distances from the pixels to their respective cluster centres, a widely used metric in unsupervised methods of commercial remote sensing software (e.g. ENVI), which can be calculated as follows:

$$M = \sum_{i=1}^m \sum_{x_j \in C_i} \|x_j - z_i\| \quad (1)$$

where  $x_j$  represents an arbitrary pixel of the image belonging to class  $i$  ( $i = 1, 2, \dots, m$ ),

with  $z_i$  as its cluster centre and  $j$  is the number of pixels in class  $i$ .

**3.2 Control parameters.** Three commonly used control parameters include the number of released artificial bees (Num\_Bee), the maximum number of iterations (Max\_Iter), and the limit of the searching time allowed (Lim\_Time) are provided for UBCO. Num\_Bee controls the number of candidate solutions, Max\_Iter provides the termination criterion for iterations, and Lim\_Time determines the number of released scouts. The parameter Lim\_Time can be computed with the following equation (Karaboga and Akay 2009):

$$\text{Lim\_Time} = \frac{1}{2} D \times \text{Num\_Bee} \quad (2)$$

where  $D$  is the dimension of the problem to be solved.

Suppose  $p$  bees are released, of which  $p / 2$  bees will be used as employed bees and the other half as unemployed bees. If a food source cannot be improved through a predefined number (Lim\_Time) of trials, then it will be abandoned and the corresponding bee will become a scout looking for food sources without any guidance.

**3.3 Food source representation.** In this paper, the cluster centre of an arbitrary class is represented with a sequence of real numbers, the number of which equals the number of attributes ( $n$ ). A food source is formed by connecting the cluster centre of each class (see Figure 3), whose length is  $n \times m$  ( $m$ , the number of classes). Here, the first  $n$  positions in the food source represent the cluster centre of class one, the second  $n$  positions represent that of class two, and so on. For example, consider a classification composed of two attributes and two classes. A food source (15.1 20.2 24.3 25.4) denotes the cluster centres (15.1 20.2) for class one and (24.3 25.4) for class two.

Figure 3 is here

**3.4 Food source initialisation.** Each employed bee is initially assigned a random food source, whose initial position can be created as follows:

$$X_i^j = X_{\min}^j + \text{rand}(0,1) (X_{\max}^j - X_{\min}^j) \quad (3)$$

where  $X_i^j$  is the position at the  $j$ th attribute for the  $i$ th bee,  $X_{\min}^j$  and  $X_{\max}^j$  is the minimum and maximum value of the  $j$ th attribute respectively, and  $\text{rand}(0,1)$  is a random value ranging from 0 to 1.

**3.5 Food source evaluation.** The profit of a food source is evaluated using the following steps:

Step 1, each pixel  $x_i, i=1, 2, \dots, N$ , is assigned to one of the clusters  $C_j$  with cluster centre  $z_j$  satisfying the equation:



$$\|X_i - z_j\| < \|X_i - z_l\|, \quad (4)$$

where  $z_l$  is the cluster center of cluster  $C_l$ ,  $j = 1, 2, \dots, m$ ,  $l = 1, 2, \dots, m$ , and  $j \neq l$ .

Step 2, considering the fact that the greater the cluster metric is the poorer the food source will be, to ensure food sources with higher nectar (lower cluster metric) possess higher profit, a profit function is defined as follows:

$$f = 1 / (M + 1), \quad (5)$$

where the cluster metric  $M$  is calculated using Equation (1).

**3.6 Food source searching of employed bee.** An employed forager, after having assessed the profit of the current food source, randomly searches for a new food source position nearby according to Equation (6), after which the profit is evaluated. If the food source has a higher nectar amount it will be chosen as her new food source.

$$V_i^j = X_i^j + \theta_i^j (X_i^j - X_k^j). \quad (6)$$

Here  $V_i^j$  is the new food source position of the  $i$ th bee at the  $j$ th attribute ( $j = 1, 2, \dots, n$ );  $X_i^j$  and  $X_k^j$  is the food source position of the  $i$ th and  $k$ th bee at the  $j$ th attribute, respectively, where  $i, k \in \{1, 2, \dots, p/2\}$  and  $k \neq i$ ;  $\theta_i^j$  is a random value ranging from -1 to 1.

**3.7 Searches for food sources by onlookers.** After each food source search, the information about the locations of nectar will be shared by employed foragers through a waggle dance. The onlookers will then choose food sources to follow, with the probability (reflecting the amount of nectar)  $P(X_i)$ , which is calculated as follows:

$$P(X_i) = \frac{f(X_i)}{\sum_{i=1}^{N_e} f(X_i)}, \quad (7)$$

where  $X_i$  is the position of the  $i$ th bee's food source,  $f(X_i)$  is the nectar amount of the food source  $X_i$ , and  $N_e$  is the number of employed bees. When initiating a search, the onlookers become employed bees to further search for food sources (Section 3.6), and much more attention can be paid to the richer food sources.

1  
2  
3 **3.8 Local and global searching for food sources.** For an employed bee, if the predefined  
4 searching time limitation (i.e. *Lim\_Time*) is reached before an improved food source is found,  
5 the current food source will be abandoned, and a new food source position will then randomly  
6 be created based on Equation (3). This initiates global searching; otherwise, food source  
7 searching (i.e. local searching) continues according to Equation (6).  
8  
9

10  
11 **3.9 Iteration termination and image classification.** When a search iteration is finished by  
12 all the bees, the best food source is recorded and compared with that of the previous iteration;  
13 the better one is chosen as the current global optimal food source. The search iteration stops  
14 when the number of maximum iterations (*Max\_Iter*) is reached, and the global optimal food  
15 source, i.e. a group of cluster centres as the solution of the unsupervised classification  
16 problem, is then obtained; otherwise, the iteration continues. Using the derived optimal food  
17 source, the image is classified and a thematic map is generated.  
18  
19

#### 20 21 **4 Study area and data**

22  
23 Zhalong National Nature Reserve (ZNNR), located on Songnen Plain of Northeast China, was  
24 built to protect existing wetland resources in 1979 and is currently of international importance  
25 by providing habitats for hundreds species of fauna and flora (Wang *et al.* 2006). The major  
26 wetland types of ZNNR are marsh (mainly in the low-lying land), meadow (mainly on plains  
27 or low-lying areas) and water. The marsh is composed of mostly *Phragmites australis* and  
28 some *Carex*, the meadow is dominated by *Tenuiflora* and *Pennisetum*, and the water consists of  
29 lake and seasonal ponds formed by the accumulation of rainwater.  
30  
31

32  
33 Figure 4 is here  
34  
35

36  
37 The test area of ZNNR, a hybrid ecosystem integrated by natural wetland and anthropic  
38 farmland, is the focus of our test site 1 (310×310 pixels; Figure 4). To further test the  
39 robustness of UBCO, two other study sites next to the ZNNR (Figure 4) with distinct  
40 landscapes were also included in this paper: site 2 (328×330 pixels) covers the Qiqihar city –  
41 an urban landscape, and site 3 (214×215 pixels) includes primarily bare soil – a natural  
42 landscape. For image classification, five categories (marsh, meadow, farmland, saline land  
43 and water) were identified in site 1, while four classes (water, road, vegetation and building)  
44 were chosen in site 2 and four classes (water, farmland, bare soil and saline land) in site 3.  
45 The classification schemes were established based on two considerations: the spectral  
46 differences among various land cover classes in the TM imagery (moderate spatial and  
47 spectral resolution) employed in this study; and the separability of vegetation classes in the  
48 context of unsupervised classification.  
49  
50

51  
52 One scene of cloudless and terrain-corrected Landsat 5 TM imagery (Row/Path: 120/27),  
53 dated on 27 August 2007, was acquired through the USGS Earth Resource Observation  
54 Systems Data Centre (<http://glovis.usgs.gov/>). The image provides 30 m spatial resolution in  
55 six multi-spectral bands (bands 1-5 and band 7) with spectral wavelengths ranging from 0.45  
56 to 2.35µm. The thermal infrared band was removed due to its unsuitability for land cover  
57 classification (Na *et al.* 2010). For geometric correction, a topographic map at the scale of  
58  
59  
60



1  
2  
3 1:50 000 that covered the imagery was acquired from the China Wetlands Science Database  
4 (<http://marsh.neigae.csdb.cn/>), on which the TM imagery was rectified and geo-referenced to  
5 the Gauss Kruger projection system using 60 ground control points evenly distributed across  
6 the image. A first order polynomial model was used for this rectification with a pixel size of  
7 30 m and root mean square (RMS) errors less than 0.5 pixels (Richards and Jia 1999).

8  
9  
10 Ground sample plots for classification accuracy validation were identified from field  
11 surveys using a hand-held GPS during the late September 2006, and a scene of high spatial  
12 resolution SPOT-5 imagery (Row/Path: 291/255) dated on 12 September 2006. A stratified  
13 random sampling was adopted to obtain an adequate number of samples for rare land cover  
14 classes (Congalton 1991, Stehman 2009). To acquire a representative sample and reduce  
15 geometric errors in image rectification and GPS reading, sample plots were collected in  
16 homogeneous regions with an area larger than about 1000 m<sup>2</sup>. For a reasonable evaluation of  
17 accuracy, the number of sample plots in each category is proportional to its area (Na *et al.*  
18 2010). In addition, plots in each category were spatially dispersed with a minimum distance  
19 of 90 m (3 pixels) to reduce spatial autocorrelation. Finally, a total of 740, 500 and 433  
20 sample plots were collected in the three study sites respectively for determining classification  
21 accuracy.  
22  
23  
24

## 25 26 27 28 29 30 31 32 33 34 35 36 37 38 39 40 41 42 43 44 45 46 47 48 49 50 51 52 53 54 55 56 57 58 59 60

### 5 Results

Similar to BCO searching for the optimal solution (a group of cluster centres) in UBCO, other  
three intelligent algorithms (GA, DE and PSO) of standardised versions were also employed  
for image clustering. For convenience, the later three image clustering methods were denoted  
as UGA, UDE and UPSO, respectively in the following text. To make a fair comparison, the  
common parameters of the four intelligent methods (UGA, UDE, UPSO and UBCO) were  
assigned with the same values, i.e. the maximum iteration number = 1000; population size =  
40. Other parameters in each of the four methods were respectively designated as follows: for  
UGA, crossover rate = 0.8, mutation rate = 0.01, generation gap=0.9; for UDE, crossover rate  
= 0.9, constant factor  $F = 0.5$ ; for UPSO, acceleration coefficients  $c_1 = c_2 = 1.8$ , inertia  
weight  $\omega = 0.6$ ; for UBCO, the value of Lim\_Time for study site 1 was 600, with 30  
variables (product of 6 attributes and 5 classes); and 480 respectively for sites 2 and 3, with  
24 variables (product of 6 attributes and 4 classes). As a benchmark, *k*-means was also  
employed with running parameters: the maximum iteration number = 1000, the pixel change  
threshold = 0%. The same reference ground data were used for classification accuracy  
evaluation of the results of five methods for the three study sites.

Figures 5, 6 and 7 illustrate the land-cover classification results of the three study sites.  
The confusion matrices and classification accuracies (overall accuracy, the producer's  
accuracy (PA) and the user's accuracy (UA)) are listed in Tables 1, 2 and 3, and the  
corresponding Kappa coefficients and their variances, as well as the Kappa Z-test (Congalton  
and Green 2008) and McNemar test (Foody 2004) results for the three classifications are  
given in Table 4. In addition, two recently proposed parameters, quantity disagreement and  
allocation disagreement, which are proved to be more useful than Kappa coefficient in  
summarizing a confusion matrix of classification (Pontius and Millones 2011), were also

1  
2  
3 calculated and are shown in Figure 8. In general, UBCO outperformed *k*-means, UGA, UDE  
4 and UPSO methods, with an increase of overall accuracy by 17%, 9%, 3% and 11%  
5 respectively for site 1 (Table 1), 7%, 4%, 1% and 1% respectively for site 2 (Table 2). For site  
6 3, improvements were 2%, 19%, 4% and 11% respectively (Table 3).  
7  
8

9  
10 Figures 5, 6, 7 and 8 are here

11  
12 For site 1 the PA and UA for meadow, saline land and water classes showed consistently high  
13 accuracy (mostly greater than 80%) throughout the classifications of five methods, due to  
14 their distinct spectral characteristics of this study site. However, the differentiation between  
15 marsh and farmland was very poor in *k*-means map (Figure 5 (b) and Table 1), due to their  
16 similar spectral characteristics, with a large number of pixels of the two classes being  
17 misclassified as each other, resulting in lower PA (21 and 71%) and UA (45 and 42%) for  
18 marsh and farmland. This poor performance of *k*-means can also be inferred from the largest  
19 total disagreement (36.90%; quantity disagreement plus allocation disagreement) of the  
20 classification (Figure 8). A notable improvement in these differentiations was observed in the  
21 UGA and UPSO classifications, but an overestimation of the marsh area occurred (Figures 5  
22 (c) and (e)). In contrast, better discrimination between marsh and farmland was achieved by  
23 UDE and UBCO, which increased UA of marsh substantially. However, it is noted that UBCO  
24 achieved better results than UDE. The total disagreement of UBCO (19.19%) decreased  
25 further in comparison with that of UDE (22.44%). The McNemar test indicated that UBCO  
26 performed significantly better than *k*-means, UGA, UDE and UPSO (Table 4).  
27  
28  
29  
30  
31

32  
33 Tables 1, 2, 3 and 4 are here

34  
35 For site 2 *k*-means (Figure 6 (b)) performed relatively poor in discriminating land cover  
36 classes. Large areas of building in *k*-means were misclassified as road, resulting in the lowest  
37 UA (50%) and PA (53%) for road and building (Table 2), respectively. Large quantity  
38 disagreements (> 16%) were also found for the classification (Figure 8). Fortunately, better  
39 and similar classification results were obtained by UGA (Figure 6 (c)), UDE (Figure 6 (d)),  
40 UPSO (Figure 6 (e)) and UBCO (Figure 6 (f)), in which road was successfully discriminated  
41 from building, despite of some overestimation. Among the four classifications, UBCO  
42 achieved the highest overall accuracy (87.80%; Table 2) and the least total disagreement  
43 (12.20%; Figure 8). Kappa Z-test further indicated that UBCO performed significantly better  
44 than *k*-means, but it presented no significant improvement over UGA, UDE and UPSO (Table  
45 4).  
46  
47

48  
49 When applied to site 3, similar but poor classification results were generated by UGA  
50 (Figure 7(c)) and UPSO (Figure 7(e)), with large areas of bare soil being misidentified as  
51 saline land, especially in the right of the map (dominated by bare soil, Figure 7(a)),  
52 demonstrating a poor PA (< 51%) in bare soil and a lower UA (< 62%) in saline land for both  
53 classifications (Table 3). Large values of total disagreement (> 24%; Figure 8) were also  
54 observed in the two classifications (UGA and UPSO). UDE performed better than UGA and  
55 UPSO, but still not good enough. However, satisfactory classification results were achieved  
56 by the rest two methods (*k*-means and UBCO) (Table 3 and Figure 7), with overall accuracies  
57  
58  
59  
60

larger than 85% and total disagreements lower than 15%. The McNemar test also suggested that *k*-means and UBCO produced statistically significantly better results than UGA, UDE and UPSO (Table 4). There was no significant difference between two best methods (*k*-means and UBCO), in spite of the slight outperformance of UBCO over *k*-means.

Figures 9 and 10 are here

To evaluate the robustness of the proposed image classification method, the five methods (*k*-means, UGA, UDE, UPSO and UBCO) were implemented 10 times for each study site. The corresponding clustering metric values and classification results (represented by the overall accuracies) are shown in Figure 9 and 10, respectively. It is clear that better and more stable clustering metric values and classification accuracies were achieved by UBCO over all the three study sites. This suggests that UBCO could consistently find the optimal or nearly optimal global solution in remote sensing image classification. In contrast, relatively poorer and less stable results were observed for *k*-means, UGA, UDE and UPSO (especially in site 1), suggesting that they were susceptible to being trapped on local optima at least in the experiments covered here.

Table 5 is here

To fairly compare the speed of the methods, the number of fitness function evaluations (FEs) (Das *et al.* 2008), instead of computing time that may be disturbed by many factors, was chosen as a measure of computational complexity. Note that all of the five methods were implemented in a MATLAB environment, and run on a personal computer with 3.20-GHz CPU and 8.0-GB memory. Table 5 shows the mean number of FEs required by the five methods for finding the optimal solution (i.e. the solution with the minimum clustering metric value after 1000 cycles) over the three study sites. As expected, due to the complex searching strategy, an obviously larger number of FEs was required by the intelligent methods in comparison with the simple *k*-means. Thereinto, UPSO had the least number of FEs, followed by UBCO, UDE and UGA.

## 6 Discussion

An unsupervised image classification can be regarded as essentially an optimization problem, which requires an optimal set of cluster centres to assign the pixels with similar features to the same class. Traditional methods (e.g. *k*-means) are constrained by the requirement that the data have certain distributions (Shah *et al.* 2004). Intelligent optimization algorithms, without such data assumptions but with a good searching ability, provide a new means of addressing image classification problems. However, common optimization methods such as genetic algorithms have difficulty finding global optimal solutions for remote sensing image classifications, due to the very large solution spaces that need to be explored and the complexity of the data. In this paper, an unsupervised bee colony optimization (UBCO) method was proposed because of its explicit and inherent global searching capacity.

The UBCO described in this paper possesses unique search strategies consisting of

1  
2  
3 exploitation and exploration processes carried out by employed bees, unemployed onlookers  
4 and scouts. In terms of exploitation (local searching), despite the increase in the proportion of  
5 promising solutions in a population (through a selection operator), UGA employs a random  
6 exploitation without special consideration of promising solutions, which can lead to slow  
7 convergence (Yen *et al.* 1998). Both UDE and UPSO adopt a greedy selection strategy  
8 between the candidate and parent solutions to exploit better ones, thereby allowing the better  
9 solutions to win the competition. But a better solution, even if the best one, can only be  
10 exploited one time in each iteration, without further seeking candidates nearby. In contrast, a  
11 hierarchical exploitation strategy is implemented by UBCO, where food sources are exploited  
12 by employed bees to yield preliminary judgments based on which richer food sources  
13 (promising solutions) are targeted and exploited by onlookers. As a result, promising regions  
14 can be searched faster and more thoroughly than with UGA, UDE and UPSO. Both UGA and  
15 UDE achieves exploration by mutating a part of a chromosome (solution) to maintain  
16 population diversity, however, the exploration range is too limited to discover new promising  
17 solution spaces (Jung 2003), which may lead to trapping on local optima. In contrast, in  
18 UBCO if a solution is proved worthless to the population, the whole solution, rather than parts  
19 of it, will be replaced by a randomly created new one by means of releasing scouts. Such a  
20 mechanism not only guarantees the diversity of the population, but also lets the final solution  
21 to be independent of the initial population, thus providing a global search capacity. Thanks to  
22 these powerful and balanced exploitation and exploration capabilities, UBCO outperformed  
23 the other four methods over all the three study sites examined here. However, we do not claim  
24 that UBCO may outperform other methods in all image clustering applications because of the  
25 complexity and diversity of remote sensing imagery.

26  
27 In comparison with the previous BCO-based unsupervised image classification methods  
28 that rely on some prior knowledge on the image (Banerjee *et al.* 2012, Deriche and Fizazi  
29 2015), the newly proposed UBCO approach has the following advantages: first, in no need of  
30 any prior knowledge, the image is classified purely based on the statistical information  
31 inherent the image; second, the image is treated as a whole, rather than pixel by pixel, by a  
32 group of cluster centres (the food source of BCO) identified by BCO itself, thus suitable to  
33 handle heterogeneous landscapes; third, only three running parameters are required in UBCO,  
34 much fewer than those of previous BCO-based methods.

35  
36 Although performed better in our experiments, UBCO is generally more computationally  
37 demanding than the simple  $k$ -means due to its complex and global searching strategies (Table  
38 5), especially in the face of large and complex data sets. Such a problem can be alleviated to  
39 some extent with the progress of modern computational techniques, such as cloud and high  
40 performance computing (Plaza and Chang 2007, Lee *et al.* 2011). In fact, speeding up the  
41 convergence of optimization algorithms by using parallel computation technology remains an  
42 active field of research (Chang *et al.* 2009, Mussi *et al.* 2011). We note that UBCO is  
43 particularly suitable for parallel computation (Narasimhan 2009), thanks to the high degree of  
44 independence between the individuals of a bee colony, and consequently improvements in  
45 convergence times might be expected.

46  
47 It is interesting to note that UBCO achieved significantly better results than the other four  
48 methods in site 1, where landscape is heterogeneous. The considerable spectral overlap  
49 among classes in the area could potentially introduce numerous sub-optimal solutions in the  
50  
51  
52  
53  
54  
55  
56  
57  
58  
59  
60

1  
2  
3 solution spaces.  $k$ -means, UGA, UDE and UPSO, with relatively weak global searching  
4 capacity, are susceptible to being trapped on such sub-optimal solutions. In contrast, UBCO is  
5 more likely to escape sub-optimal solutions and eventually approach the global optimal  
6 solution.  
7

## 8 9 **7 Conclusions and future work**

10  
11 Unsupervised image classification is a widely used method to derive land cover/use  
12 information from remote sensing imagery. However, it is a complex task and belongs to the  
13 class of NP-hard problems due to the huge solution spaces, which poses great challenges to  
14 traditional methods. Algorithms with powerful searching capabilities are urgently required for  
15 real applications. In this paper, a novel unsupervised bee colony optimization (UBCO)  
16 method is presented for remote sensing image classification. With powerful exploitation  
17 ability, UBCO can search for promising solutions rapidly and efficiently. It is less likely to  
18 become trapped on local optima than other methods, thanks to its global searching capacity.  
19 We tested UBCO in a highly heterogeneous marsh area, and compared it with  $k$ -means, UGA,  
20 UDE and UPSO methods. The preliminary experimental results reported here illustrate the  
21 superiority of UBCO over the other methods, especially dealing with the complex landscape  
22 (site 1). Hence, UBCO should be a good alternative to solve the image clustering problem.  
23

24  
25 It is well known that the choice of clustering metric exerts a great influence on results  
26 achieved by unsupervised classification methods. In addition to the Euclidean distance, other  
27 distance measurements like the spectral angle distance (measuring the angle between two  
28 spectra) should be considered to provide complementary information for pixel discrimination.  
29 We note that imagery contains much structure information that may prove valuable for land  
30 cover classification, however, how this information can be incorporated into UBCO presents a  
31 significant challenge. A BCO-based method that can automatically evolve the optimal cluster  
32 centres, as well as the number of clusters, is the next challenge for this methodology, since the  
33 number of clusters required to classify an image is generally not known *a priori* by users in  
34 most real applications. UBCO focuses on a crisp form of classification in this work, however,  
35 in consideration of the large amount of imprecision and uncertainty in remote sensing data, a  
36 fuzzy form of UBCO might be more preferable and will be investigated in future work. These  
37 issues are a priority for our future research in this field.  
38  
39

## 40 41 **Acknowledgements**

42  
43 We would like to thank the two anonymous reviewers for their constructive comments on this  
44 manuscript.  
45

## 46 47 **Funding**

48  
49 This research was supported by the National Natural Science Foundation of China (grant  
50 number: 41301465), the West Development Action Plan Program of the Chinese Academy of  
51 Sciences (grant number: KZCX2-XB3-15), the National Major Program of China (grant  
52 number: 21-Y30B05-9001-13/15-2) and the "12th Five-Year Plan" Wetland and Blackland  
53 Specialised Databases Program of the Chinese Academy of Sciences (grant number:  
54 XXH12504-3-03).  
55  
56  
57  
58  
59  
60



## References

- Adam, E., O. Mutanga, J. Odindi and E. M. Abdel-Rahman. 2014. "Land-use/cover classification in a heterogeneous coastal landscape using RapidEye imagery: evaluating the performance of random forest and support vector machines classifiers." *International Journal of Remote Sensing* 35: 3440-3458. doi:10.1080/01431161.2014.903435.
- Admane, L., K. Benatchba, M. Koudil, L. Siad and S. Maziz. 2006. "AntPart: an algorithm for the unsupervised classification problem using ants." *Applied Mathematics and Computation* 180: 16-28. doi:10.1016/j.amc.2005.11.130.
- Bagan, H., Q. X. Wang, M. Watanabe, Y. H. Yang and J. W. Ma. 2005. "Land cover classification from MODIS EVI times-series data using SOM neural network." *International Journal of Remote Sensing* 26: 4999-5012. doi:10.1080/01431160500206650.
- Banerjee, S., A. Bharadwaj, D. Gupta and V. K. Panchal. 2012. "Remote sensing image classification using artificial bee colony algorithm." *International Journal of Computer Science and Informatics* 2:67-72.
- Bartholome, E. and A. S. Belward. 2005. "GLC2000: a new approach to global land cover mapping from Earth observation data." *International Journal of Remote Sensing* 26: 1959-1977. doi:10.1080/01431160412331291297.
- Chang, Y. L., J. P. Fang, L. N. Chang, J. A. Benediktsson, H. A. Ren and K. S. Chen. 2009. "Band Selection for Hyperspectral Images Based on Parallel Particle Swarm Optimization Schemes." IGARSS09, Cape Town, South Africa, July 12-17.
- Chuvieco, E. and R. G. Congalton. 1988. "Using Cluster-Analysis to Improve the Selection of Training Statistics in Classifying Remotely Sensed Data." *Photogrammetric Engineering and Remote Sensing* 54: 1275-1281
- Cihlar, J., Q. H. Xia, J. Chen, J. Beaubien, K. Fung and R. Latifovic. 1998. "Classification by progressive generalization: A new automated methodology for remote sensing multichannel data." *International Journal of Remote Sensing* 19: 2685-2704. doi:10.1080/014311698214451.
- Congalton, R. G. 1991. "A Review of Assessing the Accuracy of Classifications of Remotely Sensed Data." *Remote Sensing of Environment* 37: 35-46. doi:10.1016/0034-4257(91)90048-B.
- Congalton, R. G., and K. Green. 2008. *Assessing the accuracy of remotely sensed data: Principles and practices (2nd ed.)*. Boca Raton, FL: CRC Press.
- Das, S., A. A. Abraham, and A. Konar. 2008. "Automatic clustering using an improved differential evolution algorithm." *Ieee Transactions on Systems Man and Cybernetics Part a-Systems and Humans* 38: 218-237. doi: 10.1109/tsmca.2007.909595.
- De Jong, K. A. 1975. *An analysis of the behavior of a class of genetic adaptive systems*. Doctoral dissertation, University of Michigan.
- Deriche, R. and H. Fizazi. 2015. "The artificial bee colony algorithm for unsupervised classification of meteorological satellite images." *International Journal of Computer Applications*, 112:28-32.
- Duda, T. and M. Canty. 2002. "Unsupervised classification of satellite imagery: choosing a good algorithm." *International Journal of Remote Sensing* 23: 2193-2212. doi:10.1080/01430060110078467.
- Fisher, P. F. 2010. "Remote sensing of land cover classes as type 2 fuzzy sets." *Remote Sensing of Environment* 114: 309-321. doi:10.1016/j.rse.2009.09.004.
- Foody, G. M. 2004. "Thematic map comparison: Evaluating the statistical significance of differences in



- classification accuracy." *Photogrammetric Engineering and Remote Sensing* 70: 627-633.
- Goncalves, M. L., M. L. A. Netto, J. a. F. Costa and J. Zullo. 2008. "An unsupervised method of classifying remotely sensed images using Kohonen self-organizing maps and agglomerative hierarchical clustering methods." *International Journal of Remote Sensing* 29: 3171-3207. doi:10.1080/01431160701442146.
- Guerschman, J. P., J. M. Paruelo, C. Di Bella, M. C. Giallorenzi and F. Pacin. 2003. "Land cover classification in the Argentine Pampas using multi-temporal Landsat TM data." *International Journal of Remote Sensing* 24: 3381-3402. doi:10.1080/0143116021000021288.
- Hong, M. H. 2011. "Multilevel thresholding selection based on the artificial bee colony algorithm for image segmentation." *Expert Systems with Applications* 38: 13785-13791. doi:10.1016/j.eswa.2011.04.180.
- Huang, Z. and S. W. Laffan. 2009. "Sensitivity analysis of a decision tree classification to input data errors using a general Monte Carlo error sensitivity model." *International Journal of Geographical Information Science* 23: 1433-1452. doi:10.1080/13658810802634949.
- Jain, A. K. 2010. "Data clustering: 50 years beyond K-means." *Pattern Recognition Letters* 31: 651-666. doi:10.1016/j.patrec.2009.09.011.
- Jain, A. K. and X. J. Yang. 2005. "Modeling the effects of two different land cover change data sets on the carbon stocks of plants and soils in concert with CO<sub>2</sub> and climate change." *Global Biogeochemical Cycles* 19. doi:10.1029/2004gb002349.
- Jung, S. H. 2003. "Queen-bee evolution for genetic algorithms." *Electronics Letters* 39: 575-576. doi: 10.1049/El:20030383.
- Karaboga, D. and B. Akay. 2009. "A comparative study of Artificial Bee Colony algorithm." *Applied Mathematics and Computation* 214: 108-132. doi:10.1016/j.amc.2009.03.090.
- Karaboga, D. and B. Basturk. 2007. "A powerful and efficient algorithm for numerical function optimization: artificial bee colony (ABC) algorithm." *Journal of Global Optimization* 39: 459-471. doi:10.1007/s10898-007-9149-x.
- Karaboga, D. and B. Basturk. 2008. "On the performance of artificial bee colony (ABC) algorithm." *Applied Soft Computing* 8: 687-697. doi:10.1016/j.asoc.2007.05.007.
- Karaboga, D., B. Gorkemli, C. Ozturk and N. Karaboga. 2014. "A comprehensive survey: artificial bee colony (ABC) algorithm and applications." *Artificial Intelligence Review* 42: 21-57. doi:10.1007/s10462-012-9328-0.
- Kerr, J. T. and M. Ostrovsky. 2003. "From space to species: ecological applications for remote sensing." *Trends in Ecology & Evolution* 18: 299-305. doi: 10.1016/S0169-5347(03)00071-5.
- Khan, S. S. and A. Ahmad. 2004. "Cluster center initialization algorithm for K-means clustering." *Pattern Recognition Letters* 25: 1293-1302. doi:10.1016/j.patrec.2004.04.007.
- Lee, C. A., S. D. Gasster, A. Plaza, C. I. Chang and B. Huang. 2011. "Recent Developments in High Performance Computing for Remote Sensing: A Review." *Ieee Journal of Selected Topics in Applied Earth Observations and Remote Sensing* 4: 508-527. doi: 10.1109/Jstars.2011.2162643.
- Li, H.P., S.Q. Zhang, X.H. Ding, C. Zhang and P. Dale. 2016. "Performance Evaluation of Cluster Validity Indices (CVIs) on Multi/Hyperspectral Remote Sensing Datasets." *Remote Sensing* 8: 295. doi: 10.3390/rs8040295.
- Liu, X. P., X. Li, L. Liu, J. Q. He and B. Ai. 2008. "An Innovative Method to Classify Remote-Sensing Images Using Ant Colony Optimization." *Ieee Transactions on Geoscience and Remote Sensing* 46: 4198-4208. doi:10.1109/Tgrs.2008.2001754.

- 1  
2  
3 Lu, D. and Q. Weng. 2007. "A survey of image classification methods and techniques for improving  
4 classification performance." *International Journal of Remote Sensing* 28: 823-870.  
5 doi:10.1080/01431160600746456.  
6
- 7 Maulik, U. and S. Bandyopadhyay. 2000. "Genetic algorithm-based clustering technique." *Pattern  
8 Recognition* 33: 1455-1465. doi:10.1016/S0031-3203(99)00137-5.  
9
- 10 Melgani, F. and L. Bruzzone. 2004. "Classification of hyperspectral remote sensing images with  
11 support vector machines." *Ieee Transactions on Geoscience and Remote Sensing* 42: 1778-1790.  
12 doi:10.1109/Tgrs.2004.831865.
- 13 Miller, J. D. and S. R. Yool. 2002. "Mapping forest post-fire canopy consumption in several overstory  
14 types using multi-temporal Landsat TM and ETM data." *Remote Sensing of Environment* 82:  
15 481-496. doi:Pii S0034-4257(02)00071-8.  
16
- 17 Mussi, L., F. Daolio and S. Cagnoni. 2011. "Evaluation of parallel particle swarm optimization  
18 algorithms within the CUDA (TM) architecture." *Information Sciences* 181: 4642-4657. doi:  
19 10.1016/j.ins.2010.08.045.
- 20 Na, X. D., S. Q. Zhang, X. F. Li, H. A. Yu and C. Y. Liu. 2010. "Improved Land Cover Mapping using  
21 Random Forests Combined with Landsat Thematic Mapper Imagery and Ancillary Geographic  
22 Data." *Photogrammetric Engineering and Remote Sensing* 76: 833-840.  
23
- 24 Narasimhan, H. 2009. "Parallel Artificial Bee Colony (PABC) Algorithm." NaBIC09, Coimbatore,  
25 India, Decemeber 9-11.  
26
- 27 Otukey, J. R. and T. Blaschke. 2010. "Land cover change assessment using decision trees, support  
28 vector machines and maximum likelihood classification algorithms." *International Journal of  
29 Applied Earth Observation and Geoinformation* 12: S27-S31. doi:10.1016/j.jag.2009.11.002.  
30
- 31 Pal, M. 2008. "Artificial immune-based supervised classifier for land-cover classification."  
32 *International Journal of Remote Sensing* 29: 2273-2291. doi:10.1080/01431160701408402.  
33
- 34 Plaza, A. J. and C. I. Chang. 2008. *High performance computing in remote sensing*. Gainesville, USA:  
35 CRC Press.
- 36 Pontius, R. G. and M. Millones. 2011. "Death to Kappa: birth of quantity disagreement and allocation  
37 disagreement for accuracy assessment." *International Journal of Remote Sensing* 32: 4407-4429.  
38 doi:10.1080/01431161.2011.552923.  
39
- 40 Price, K., R. Storn and A. Lampinen. 2005. *Differential Evolution a Practical Approach to Global  
41 Optimization*. Berlin: Springer.
- 42 Richards, J. and X. Jia. 1999. *Remote Sensing Digital Image Analysis*. Berlin: Springer.
- 43 Schmid, T., M. Koch, J. Gumuzzio and P. M. Mather. 2004. "A spectral library for a semi-arid wetland  
44 and its application to studies of wetland degradation using hyperspectral and multispectral data."  
45 *International Journal of Remote Sensing* 25: 2485-2496. doi:10.1080/0143116031000117001.  
46
- 47 Shah, C. A., M. K. Arora and P. K. Varshney. 2004. "Unsupervised classification of hyperspectral data:  
48 an ICA mixture model based approach." *International Journal of Remote Sensing* 25: 481-487.  
49 doi:10.1080/01431160310001618040.  
50
- 51 Shukran, M. A., Y. Y. Chung, W. Yeh, N. Wahid and A. M. Zaidi. 2011. "Artificial bee colony based  
52 data mining algorithms for classification tasks." *Modern Applied Science* 5: 217-231.  
53 doi:10.5539/mas.v5n4p217.  
54
- 55 Stehman, S. V. 2009. "Sampling designs for accuracy assessment of land cover." *International Journal  
56 of Remote Sensing* 30: 5243-5272. doi:10.1080/01431160903131000.  
57
- 58 Storn, P. and K. Price. 1995. "Differential evolution – a simple and efficient adaptive scheme for global  
59  
60

- 1  
2  
3 optimization over continuous spaces. " *Technical Report*, Berkley, International Computer Science  
4 Institute.
- 5 Wang, H., S. G. Xu and L. S. Sun. 2006. "Effects of Climatic Change on Evapotranspiration in  
6 Zhalong Wetland, Northeast China." *Chinese Geographical Science* 16: 265-269.  
7 doi:10.1007/s11769-006-0265-1.
- 8  
9  
10 Wong, L. P., M. Y. H. Low and C. S. Chong. 2010. "Bee Colony Optimization with Local Search for  
11 Traveling Salesman Problem." *International Journal on Artificial Intelligence Tools* 19: 305-334.  
12 doi:10.1142/S0218213010000200.
- 13 Wright, C. and A. Gallant. 2007. "Improved wetland remote sensing in Yellowstone National Park  
14 using classification trees to combine TM imagery and ancillary environmental data." *Remote*  
15 *Sensing of Environment* 107: 582-605. doi:10.1016/j.rse.2006.10.019.
- 16  
17 Xiao, X. M., S. Boles, J. Y. Liu, D. F. Zhuang and M. L. Liu. 2002. "Characterization of forest types in  
18 Northeastern China, using multi-temporal SPOT-4 VEGETATION sensor data." *Remote Sensing of*  
19 *Environment* 82: 335-348. doi:Pii S0034-4257(02)00051-2.
- 20  
21 Yen, J., J. C. Liao, B. J. Lee and D. Randolph. 1998. "A hybrid approach to modeling metabolic  
22 systems using a genetic algorithm and simplex method." *Ieee Transactions on Systems Man and*  
23 *Cybernetics Part B-Cybernetics* 28: 173-191. doi: 10.1109/3477.662758.
- 24  
25  
26  
27  
28  
29  
30  
31  
32  
33  
34  
35  
36  
37  
38  
39  
40  
41  
42  
43  
44  
45  
46  
47  
48  
49  
50  
51  
52  
53  
54  
55  
56  
57  
58  
59  
60

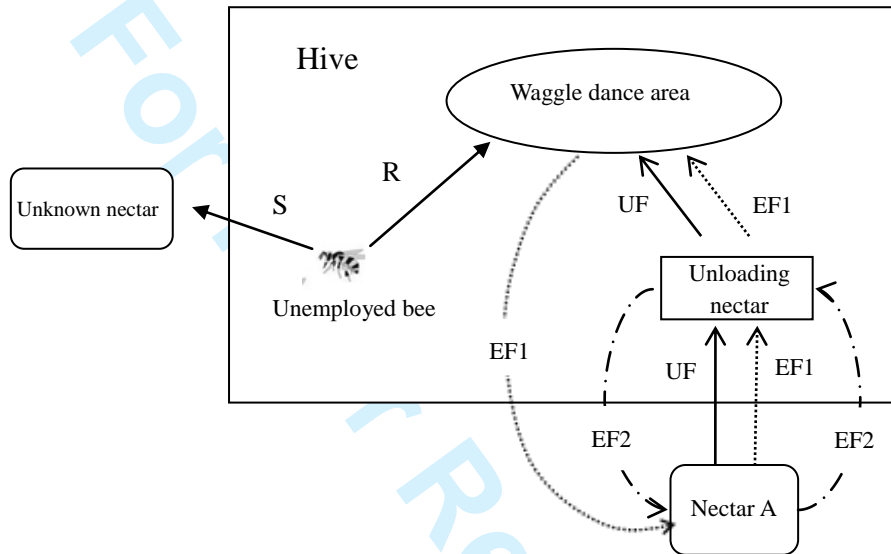


Figure 1. The behaviours exhibited by bees when searching for nectar. UF indicates an uncommitted follower; EF1 identifies the first class of employed forager and EF2 the second class of employed forager. R denotes an unemployed bee recruited by an employed forager, and S denotes an unemployed bee randomly searching for a food source.

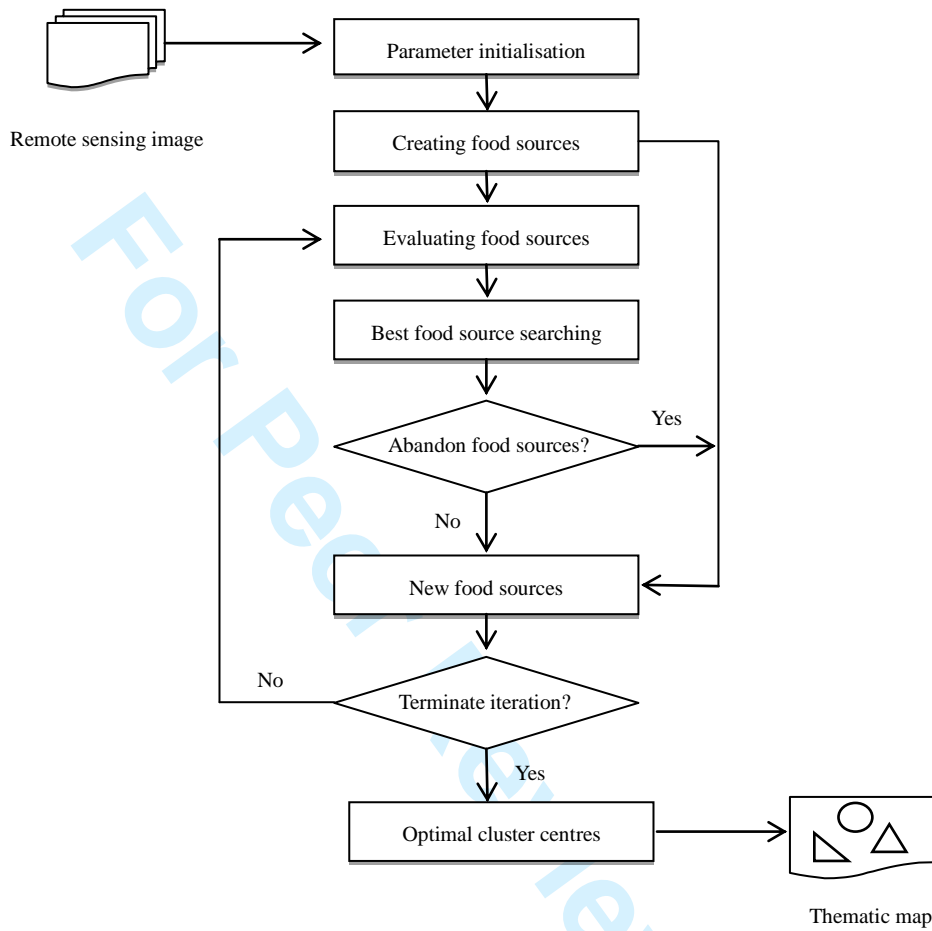


Figure 2. Flowchart of UBCO for remote sensing image classification.

1  
2  
3  
4  
5  
6  
7  
8  
9  
10  
11  
12  
13  
14  
15  
16  
17  
18  
19  
20  
21  
22  
23  
24  
25  
26  
27  
28  
29  
30  
31  
32  
33  
34  
35  
36  
37  
38  
39  
40  
41  
42  
43  
44  
45  
46  
47  
48  
49  
50  
51  
52  
53  
54  
55  
56  
57  
58  
59  
60

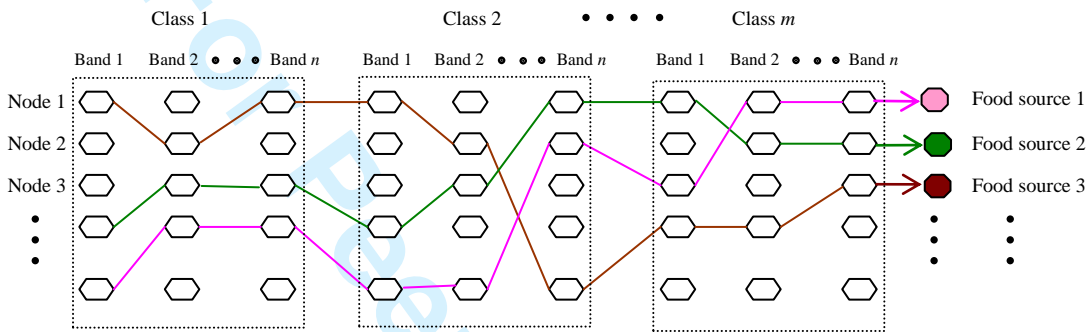


Figure 3. The formation of food sources from cluster centres in UBCO, where nodes are arbitrary DN values of remote sensing image.



1  
2  
3  
4  
5  
6  
7  
8  
9  
10  
11  
12  
13  
14  
15  
16  
17  
18  
19  
20  
21  
22  
23  
24  
25  
26  
27  
28  
29  
30  
31  
32  
33  
34  
35  
36  
37  
38  
39  
40  
41  
42  
43  
44  
45  
46  
47  
48  
49  
50  
51  
52  
53  
54  
55  
56  
57  
58  
59  
60

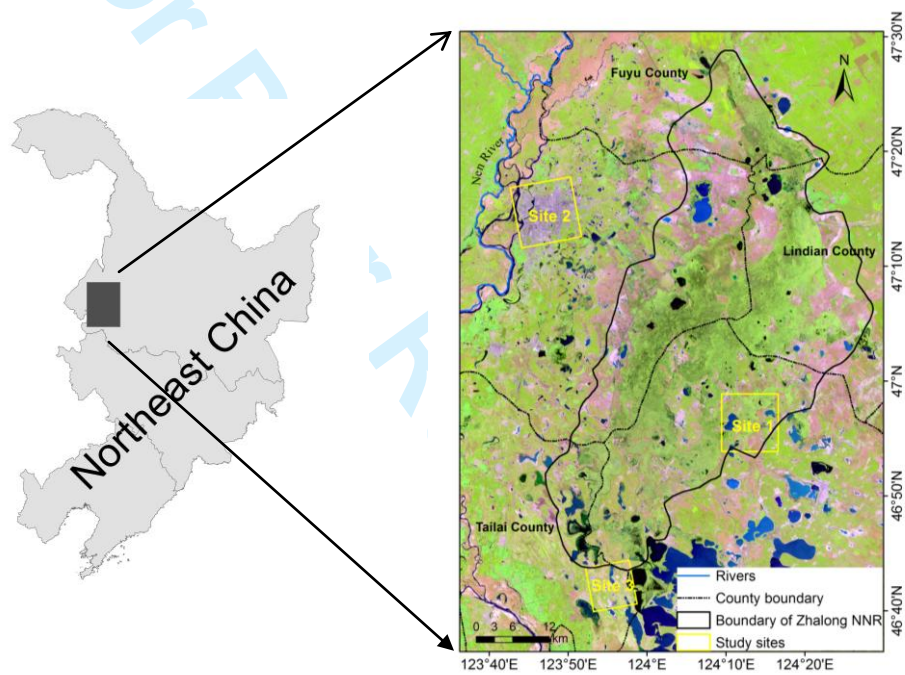


Figure 4. Location of the three study sites.

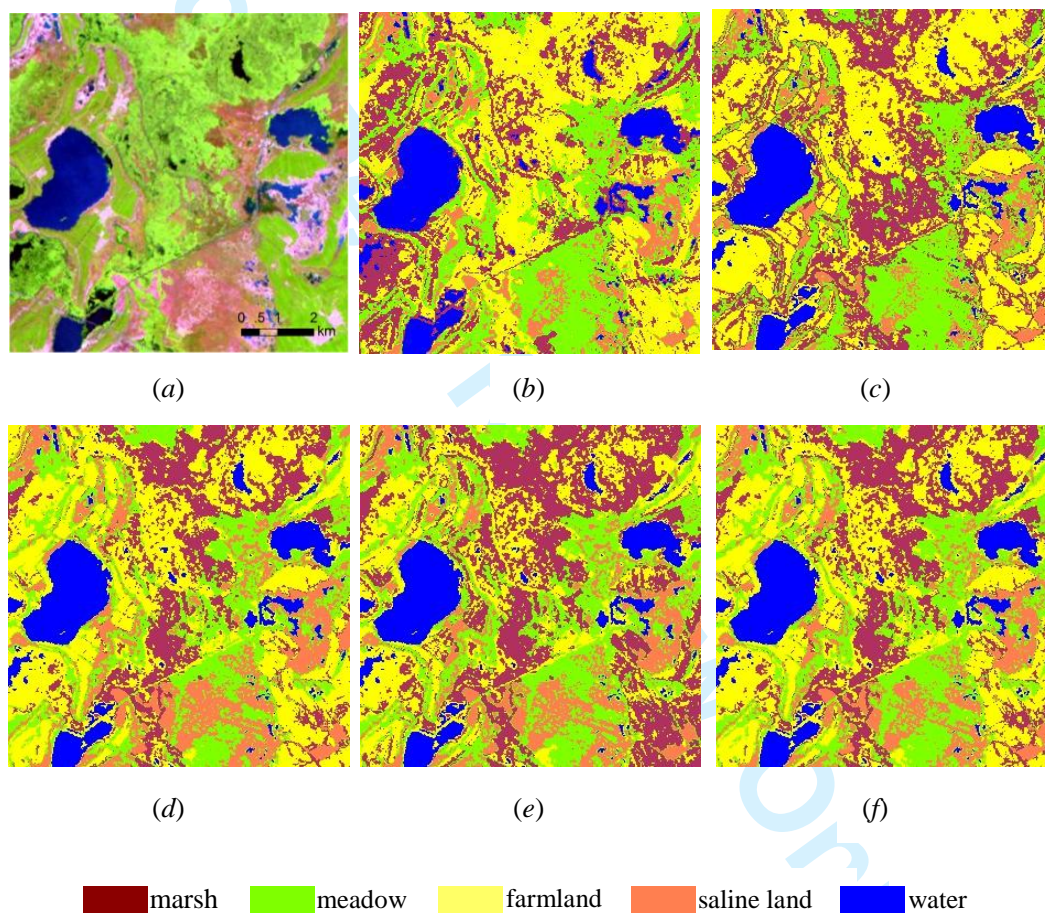


Figure 5. TM image and classification maps of the five methods of study site 1 (a) TM image (bands 5, 4, 3) (b-f) classification maps generated by *k-means*, UGA, UDE, UPSO and UBCO methods, respectively.



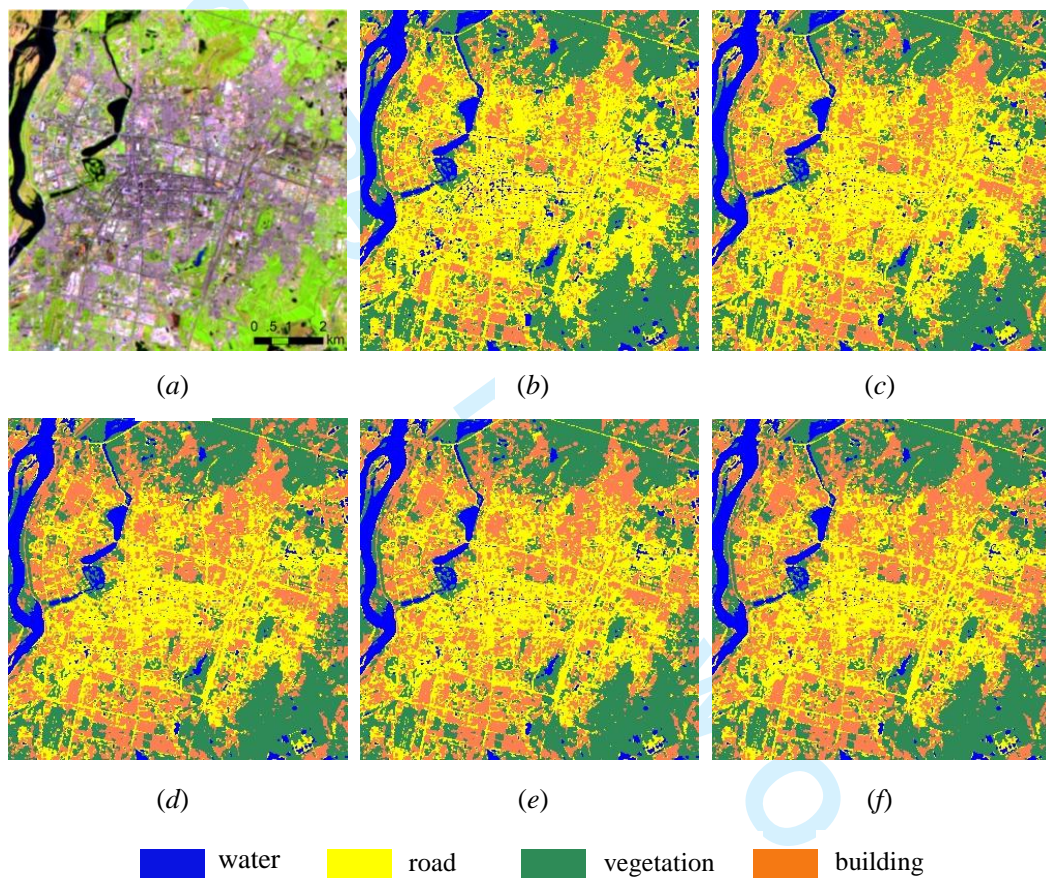


Figure 6. TM image and classification maps of the five methods of study site 2 (a) TM image (bands 5, 4, 3) (b-f) classification maps generated by **k-means**, UGA, UDE, UPSO and UBCO methods, respectively.

1  
2  
3  
4  
5  
6  
7  
8  
9  
10  
11  
12  
13  
14  
15  
16  
17  
18  
19  
20  
21  
22  
23  
24  
25  
26  
27  
28  
29  
30  
31  
32  
33  
34  
35  
36  
37  
38  
39  
40  
41  
42  
43  
44  
45  
46  
47  
48  
49  
50  
51  
52  
53  
54  
55  
56  
57  
58  
59  
60

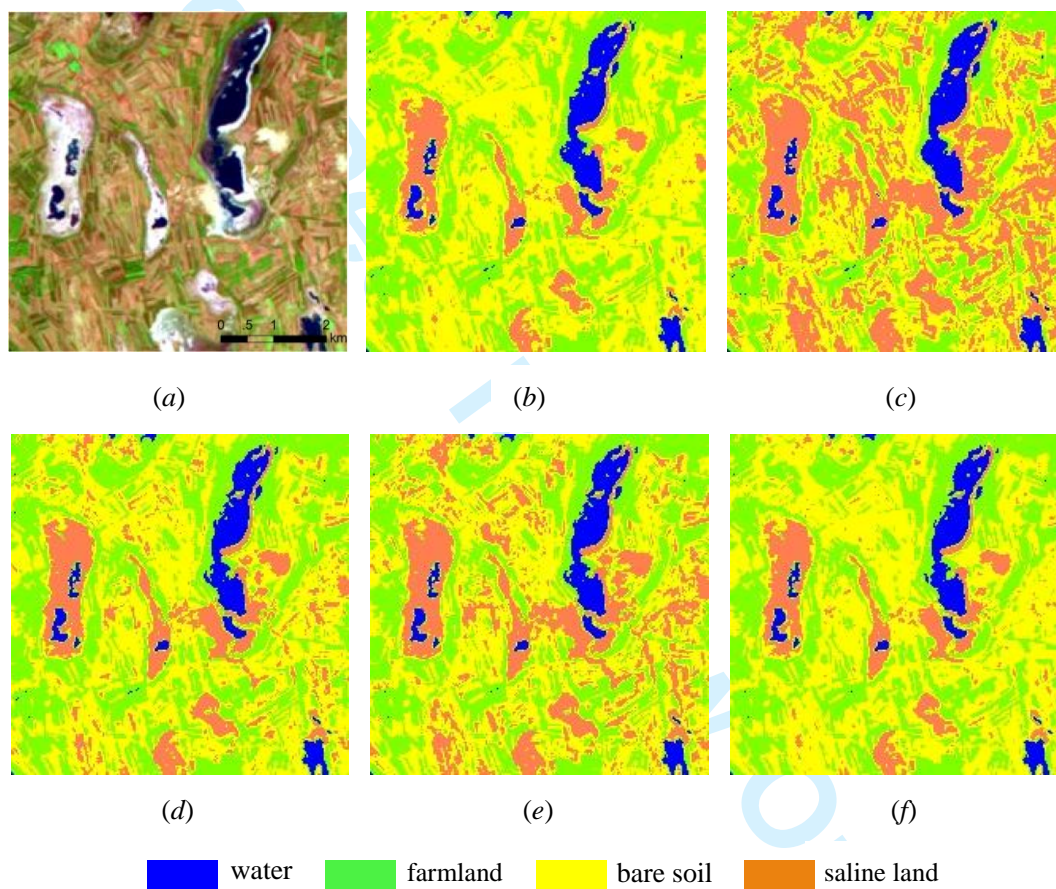


Figure 7. TM image and classification maps of the five methods of study site 3 (a) TM image (bands 5, 4, 3) (b-f) classification maps generated by *k-means*, UGA, UDE, UPSO and UBCO methods, respectively.

1  
2  
3  
4  
5  
6  
7  
8  
9  
10  
11  
12  
13  
14  
15  
16  
17  
18  
19  
20  
21  
22  
23  
24  
25  
26  
27  
28  
29  
30  
31  
32  
33  
34  
35  
36  
37  
38  
39  
40  
41  
42  
43  
44  
45  
46  
47  
48  
49  
50  
51  
52  
53  
54  
55  
56  
57  
58  
59  
60

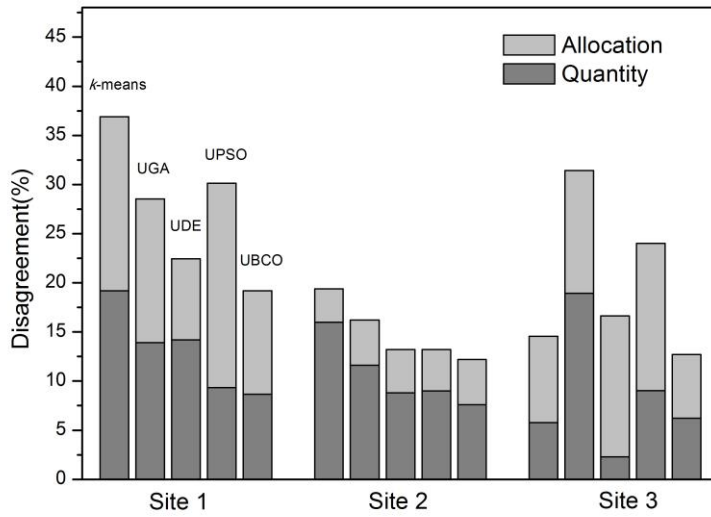


Figure 8. Quantity disagreement and allocation disagreement for confusion matrices of the classifications in this paper.

1  
2  
3  
4  
5  
6  
7  
8  
9  
10  
11  
12  
13  
14  
15  
16  
17  
18  
19  
20  
21  
22  
23  
24  
25  
26  
27  
28  
29  
30  
31  
32  
33  
34  
35  
36  
37  
38  
39  
40  
41  
42  
43  
44  
45  
46  
47  
48  
49  
50  
51  
52  
53  
54  
55  
56  
57  
58  
59  
60

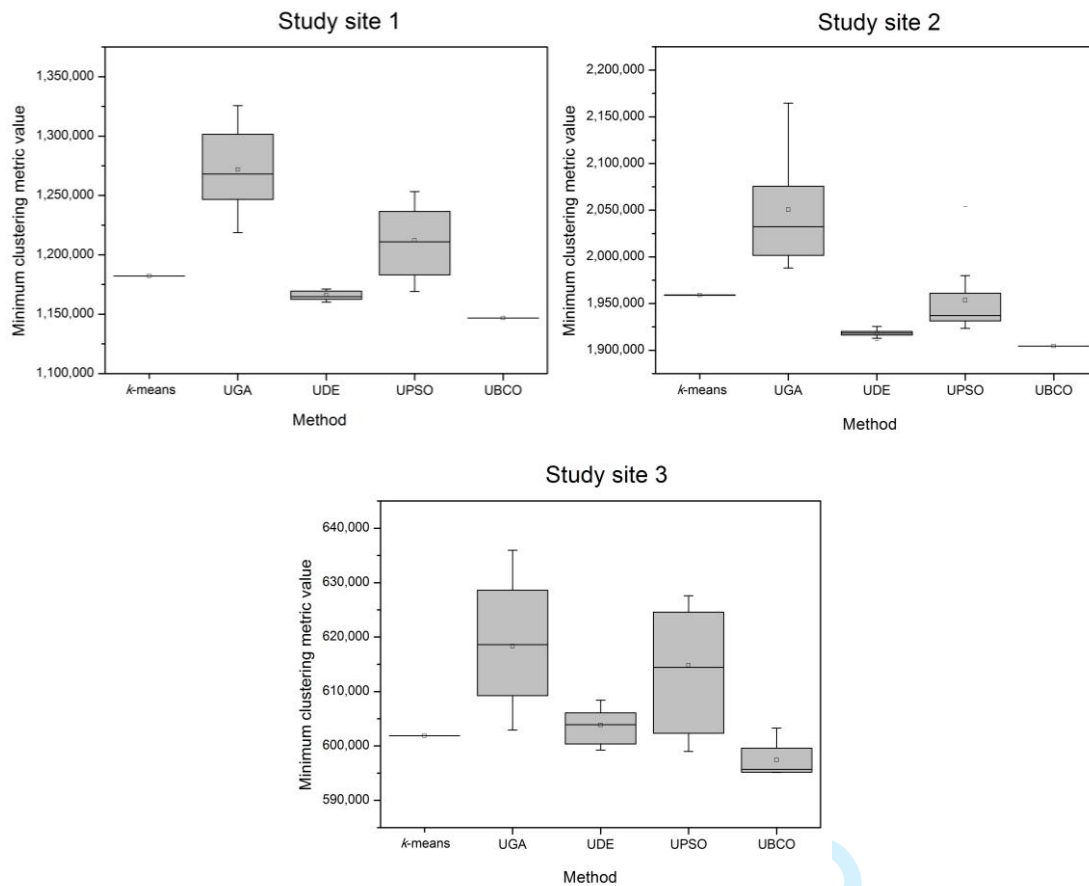


Figure 9. Box plots of the minimum clustering metric values for the five methods applied to the three study sites.



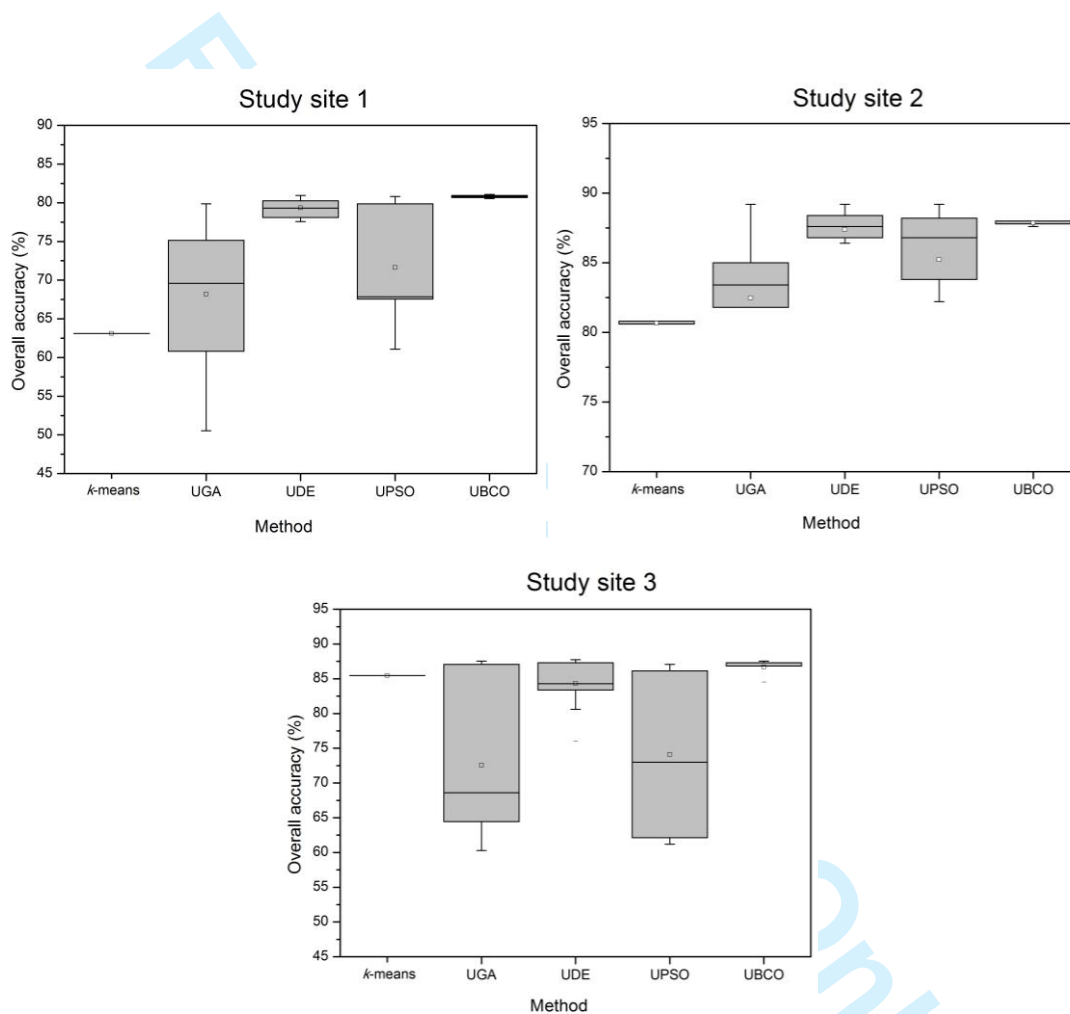


Figure 10. Box plots of overall accuracies for the five methods applied to the three study sites.

Table 1. Confusion matrices of classification results achieved by the five methods in study site 1.

Method	Reference data							
	Classified data	Marsh	Meadow	Farmland	Saline land	Water	Total	UA (%)
<i>k</i> -means	Marsh	49	7	53	0	0	109	44.95
	Meadow	0	114	3	19	0	136	83.82
	Farmland	186	0	137	0	0	323	42.41
	Saline land	0	4	0	88	0	92	95.65
	Water	1	0	0	0	79	80	98.75
	Total	236	125	193	107	79	740	
	PA (%)	20.76	91.20	70.98	82.24	100.00		
Overall accuracy = 63.11%								
UGA	Marsh	108	19	33	0	0	160	67.50
	Meadow	0	103	0	28	0	131	78.63
	Farmland	127	2	160	0	0	289	55.36
	Saline land	0	1	0	79	0	80	98.75
	Water	1	0	0	0	79	80	98.75
	Total	236	125	193	107	79	740	
	PA (%)	45.76	82.40	82.90	73.83	100.00		
Overall accuracy = 71.49%								
UDE	Marsh	136	0	20	0	0	156	87.18
	Meadow	1	89	7	3	0	100	89.00
	Farmland	98	4	166	0	0	268	61.94
	Saline land	0	32	0	104	0	136	76.47
	Water	1	0	0	0	79	80	98.75
	Total	236	125	193	107	79	740	
	PA (%)	57.63	71.20	86.01	97.20	100.00		
Overall accuracy = 77.57%								
UPSO	Marsh	173	0	122	0	0	295	58.64
	Meadow	1	103	7	9	0	120	85.83
	Farmland	61	4	64	0	0	129	49.61
	Saline land	0	18	0	98	0	116	84.48
	Water	1	0	0	0	79	80	98.75
	Total	236	125	193	107	79	740	
	PA (%)	73.31	82.40	33.16	91.59	100.00		
Overall accuracy = 69.86%								
UBCO	Marsh	149	0	26	0	0	175	85.14
	Meadow	0	109	5	8	0	122	89.34
	Farmland	86	4	162	0	0	252	64.29
	Saline land	0	12	0	99	0	111	89.19
	Water	1	0	0	0	79	80	98.75
	Total	236	125	193	107	79	740	
	PA (%)	63.14	87.20	83.94	92.52	100.00		
Overall accuracy = 80.81%								

Note: PA and UA represent the producer's accuracy and the user's accuracy, respectively.

Table 2. Confusion matrices of classification results achieved by the five methods in study site 2.

Method	Classified data	Reference data					Total	UA (%)
		Water	Road	Vegetation	Building			
<i>k</i> -means	Water	103	4	0	1	108	95.37	
	Road	0	84	4	79	167	50.30	
	Vegetation	0	2	125	1	128	97.66	
	Building	0	2	4	91	97	93.81	
	Total	103	92	133	172	500		
	PA (%)	100.00	91.30	93.98	52.91			
Overall accuracy = 80.60%								
UGA	Water	103	0	0	0	103	100.00	
	Road	0	83	19	48	150	55.33	
	Vegetation	0	2	109	0	111	98.20	
	Building	0	7	5	124	136	91.18	
	Total	103	92	133	172	500		
	PA (%)	100.00	90.22	81.95	72.09			
Overall accuracy = 83.80%								
UDE	Water	103	0	0	0	103	100.00	
	Road	0	84	3	49	136	61.76	
	Vegetation	0	2	125	1	128	97.66	
	Building	0	6	5	122	133	91.73	
	Total	103	92	133	172	500		
	PA (%)	100.00	91.30	93.98	70.93			
Overall accuracy = 86.80%								
UPSO	Water	103	0	0	0	103	100.00	
	Road	0	84	3	50	137	61.31	
	Vegetation	0	2	125	0	127	98.43	
	Building	0	6	5	122	133	91.73	
	Total	103	92	133	172	500		
	PA (%)	100.00	91.30	93.98	70.93			
Overall accuracy = 86.80%								
UBCO	Water	103	0	0	0	103	100.00	
	Road	0	83	3	44	130	63.85	
	Vegetation	0	1	125	0	126	99.21	
	Building	0	8	5	128	141	90.78	
	Total	103	92	133	172	500		
	PA (%)	100.00	90.22	93.98	74.42			
Overall accuracy = 87.80%								

Note: PA and UA represent the producer's accuracy and the user's accuracy, respectively.

Table 3. Confusion matrices of classification results achieved by the five methods in study site 3.

Method	Classified data	Reference data					Total	UA (%)
		Water	Farmland	Bare soil	Saline land			
<i>k</i> -means	Water	70	8	0	0	78	89.74	
	Farmland	5	108	11	3	127	85.04	
	Bare soil	1	7	114	25	147	77.55	
	Saline land	0	0	3	78	81	96.30	
	Total	76	123	128	106	433		
	PA (%)	92.11	87.80	89.06	73.58			
Overall accuracy = 85.45%								
UGA	Water	71	13	0	0	84	84.52	
	Farmland	3	95	2	1	101	94.06	
	Bare soil	2	14	39	13	68	57.35	
	Saline land	0	1	87	92	180	51.11	
	Total	76	123	128	106	433		
	PA (%)	93.42	77.24	30.47	86.79			
Overall accuracy = 68.59%								
UDE	Water	69	6	0	0	75	92.00	
	Farmland	6	111	12	3	132	84.09	
	Bare soil	0	5	96	18	119	80.67	
	Saline land	1	1	20	85	107	79.44	
	Total	76	123	128	106	433		
	PA (%)	90.79	90.24	75.00	80.19			
Overall accuracy = 83.37%								
UPSO	Water	69	6	0	0	75	92.00	
	Farmland	5	107	9	3	124	86.29	
	Bare soil	1	9	65	15	90	72.22	
	Saline land	1	1	54	88	144	61.11	
	Total	76	123	128	106	433		
	PA (%)	90.79	86.99	50.78	83.02			
Overall accuracy = 75.98%								
UBCO	Water	69	2	0	0	71	97.18	
	Farmland	6	114	11	3	134	85.07	
	Bare soil	1	7	114	22	144	79.17	
	Saline land	0	0	3	81	84	96.43	
	Total	76	123	128	106	433		
	PA (%)	90.79	92.68	89.06	76.42			
Overall accuracy = 87.30%								

Note: PA and UA represent the producer's accuracy and the user's accuracy, respectively.

Table 4. The Kappa coefficients and their variances, as well as the Kappa Z-test and McNemar test results (bold numbers: significant difference at 95% confidence level).

Study site	Method	Kappa coefficient		Z-value			
		Value	Variance ( $\times 10^{-4}$ )	UGA	UDE	UPSO	UBCO
Site 1	<i>k</i> -means	0.5262	5.4592	<b>3.1377/3.9584</b>	<b>5.6953/6.7917</b>	<b>2.3959/3.3314</b>	<b>7.0704/8.2863</b>
	UGA	0.6307	5.6331	-	<b>2.4615/4.6664</b>	0.7165/0.2046	<b>3.7707/7.0618</b>
	UDE	0.7114	5.1152	-	-	<b>3.1790/4.0291</b>	1.3011/4.3519
	UPSO	0.6065	5.7736	-	-	-	<b>4.4908/6.6034</b>
	UBCO	0.7523	4.7669	-	-	-	-
Site 2	<i>k</i> -means	0.7445	7.6324	1.0240/ <b>4.1461</b>	<b>2.1198/5.4272</b>	<b>2.1202/5.1257</b>	<b>2.4924 /5.1962</b>
	UGA	0.7839	7.1715	-	1.0807/ <b>3.4000</b>	1.0809/ <b>3.0000</b>	1.4486/ <b>3.1568</b>
	UDE	0.8235	6.2561	-	-	0.0000/1.4142	0.3690/0.0000
	UPSO	0.8235	6.2518	-	-	-	0.3691/1.0000
	UBCO	0.8364	5.9631	-	-	-	-
Site 3	<i>k</i> -means	0.8031	7.9504	<b>5.0947/6.3791</b>	0.6732/ <b>2.0426</b>	<b>2.9328/3.8730</b>	0.6331/1.8974
	UGA	0.5821	10.8661	-	<b>4.3860/5.6335</b>	<b>2.0800/4.7646</b>	<b>5.7694/6.7625</b>
	UDE	0.7757	8.6173	-	-	<b>2.2507/3.0424</b>	1.3071/ <b>3.5447</b>
	UPSO	0.6778	10.3030	-	-	-	<b>3.5782/4.8107</b>
	UBCO	0.8278	7.2702	-	-	-	-

Note: 'Z-value' denotes either the kappa **Z-test** value or the McNemar test result.



Table 5. The mean number of fitness function evaluations required by the five methods over the three study sites.

Study site	Mean number of fitness function evaluations				
	<i>k</i> -means	UGA	UDE	UPSO	UBCO
Site 1	348	198480	176904	50640	167800
Site 2	291	158672	141091	50128	99808
Site 3	111	158208	136210	33664	144064